PCCP

Spin Manipulation with Magnetic Semiconductor Barriers

Journal:	*Physical Chemistry Chemical Physics*
Manuscript ID:	CP-PER-10-2014-004599.R1
Article Type:	Perspective
Date Submitted by the Author:	11-Nov-2014
Complete List of Authors:	Moodera, Jagadeesh S.; MIT, Physics Miao, Guoxing; University of Waterloo, Electrical Engineering Department

Spin Manipulation with Magnetic Semiconductor Barriers

Guo-Xing Miao,[1] and Jagadeesh S. Moodera,[2,3]

[1]Institute for Quantum Computing and Department of Electrical and Computer Engineering, University of Waterloo, Waterloo, Ontario, Canada N2L3G1

[2]Francis Bitter Magnet Laboratory, [3]Department of Physics, Massachusetts Institute of Technology, Cambridge, Massachusetts 02139, USA

Abstract: Magnetic semiconductors are a class of materials with special spin-filtering capabilities with their magnetically tunable energy gaps. Many of these materials also possess another intrinsic property: indirect exchange interaction between the localized magnetic moments and the adjacent free electrons, which manifests as an extremely large effective magnetic field applying only on the free electrons' spin degrees of freedom. Novel device concepts can be created by taking advantage of these properties. We discuss in the article the basic principles of these phenomena, and potential ways of applying them in constructing spintronic devices.

I. Spin Filtering

Magnetic semiconductors are best known for their spin filtering capabilities. The phenomena were first proposed as a method to generate spin-polarized electron beam on field emission electron guns [1,2]. Because of the existence of the finite band gap between the conduction band and the valence band, electron transport through these materials can only take place through quantum mechanical tunneling, provided that the temperature is not too high to overcome the band gap. The transport becomes spin-dependent when the material goes through its ferromagnetic transition, and the presence of exchange interaction leads to spin asymmetry for the two spin channels. When unpolarized electrons tunnel across such a spin dependent tunnel barrier, electrons of different spins encounter different tunnel barrier heights and therefore cross with different probability, thus the transient current becomes spin polarized. These materials are termed "spin-filters" due to the active spin selectivity of the tunnel process [3,4]. In principle, all ferro- and ferri-magnetic semiconductors or insulators have such spin-filter capability, and the filtering efficiency is a function of the magnitude of exchange splitting, and the tunnel barrier thickness. These are easy to understand from a simple quantum mechanical tunneling picture (Fig.1): the electrons' tunnel probability is exponentially dependent on the tunnel barrier height and thickness. For a simple nonmagnetic energy barrier such as Al_2O_3, no spin selectivity happens and all electrons cross the barrier at the same rate. Now that the barrier is made out of a magnetic material, the up and down electrons will encounter different tunnel barrier heights and the transport become spin-dependent. And with the exponential dependence of tunnel probability on the energy barrier heights, a small exchange splitting on the barrier heights leads to dramatic difference in the transport probability for the two spin channels. When the barrier is thick enough, the minority electrons (minority with respect to the barrier) are essentially filtered out from the

stream, and the net tunnel current becomes nearly 100% spin polarized. Experimentally, one can directly measure spin polarization across a spin filter with superconducting Meservey-Tedrow technique [5], where the tunnel currents' spin polarization manifests as an imbalance of tunnel conductance on the two spin channels, and readily resolvable when the superconductor-magnetic semiconductors-normal metal tunnel junction is subject to a strong in-plane Zeeman field. For example, 29% spin polarization across EuO [6], 85% across EuS [7,8], 26% across $CoFe_2O_4$ [9], and 9% across $MnFe_2O_4$ [10], were reported in the literature. A closely related technique, Point Contact Andreev reflection (PCAR) [11] of superconducting Cooper pairs, also probes the local availability of spin carriers and can be used to evaluate the spin filter efficiency. For example, 13% was reported for $CoFe_2O_4$ barriers [12]. A major drawback of the above techniques is that they are limited to superconducting temperatures only, typically below 1 K. The spin polarization can also be deduced indirectly, for example, through temperature dependence of the tunnel resistance across a spin filter (98% across EuO [13], 90% across GdN [14], 75% across $Sm_{0.75}Sr_{0.25}MnO_3$ [15]), or from magnetoresistance (MR) measurement on single and double spin filter tunnel junctions (40-90% across EuS [16,17,18], 25% across EuO [19], 22% across $NiFe_2O_4$ [20], 22% across $BiMnO_3$ [21], 20-30% across $Pr_{0.8}Ca_{0.2}Mn_{1-y}Co_yO_3$ (PCMCO) [22], negative and up to -44% across $CoFe_2O_4$ [23,24,25]). The above examples include some of the most popular spin filter materials, such as rear-earth compounds, ferrites and manganites. We notice quite some discrepancy on the estimation with different methods: more complicated device structure tends to yield lower spin filter efficiency. This is because the imperfections on the materials themselves and the interfaces between them both go up with device complexity. To date, room temperature operation of spin-filtering remains a big challenge, no more than a few percent spin filter efficiency has been achieved and only on ferrite systems thus far [23,24,25]. This is in part due

to the intrinsic low Curie temperature of many of the materials (such as the rare-earth compounds and many manganites), and in part due to the difficulty of creating high quality materials (such as the ferrites). Defects within a barrier tend to induce resonant transport bypassing the spin filter barriers and result in much reduced spin filter efficiency [9]. At room temperature these defect-mediated channels become dominant and mask the desired spin filter contributions. The observed spin filtering efficiencies are negative in these ferrite systems, consistent with first-principles theoretical expectations [26,27]. There has been a claim of positive spin filtering efficiency exceeding 70% at room temperature, on $CoFe_2O_4/MgAl_2O_4/Fe_3O_4$ tunnel junctions measured with conducting AFM (atomic force microscopy) [28]. The half-metallicity and negative spin polarization of Fe_3O_4 may not have been correctly accounted for in this work with the limited analysis.

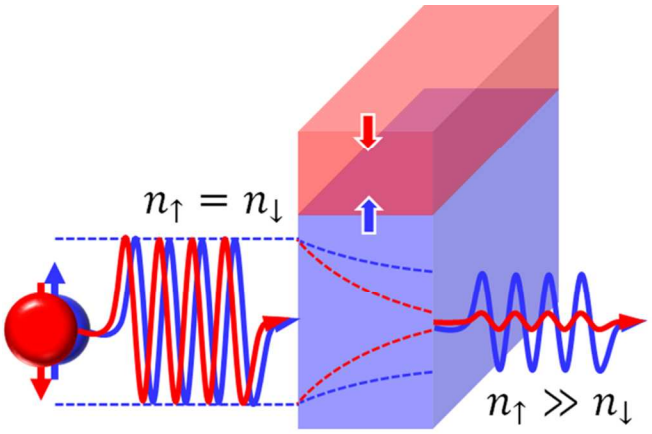

Fig.1 Illustration of spin filtering process across a magnetic barrier, where the spin-up barrier height (blue) is lower than the spin-down barrier height (red). The amplitude of an incoming plane wave is more attenuated if the spins are pointing downward, opposite to the majority bands of the spin filter barrier.

In addition to creating a highly polarized spin current from an unpolarized charge current, the spin-filters can also function as efficient spin detectors due to their spin selectivity. The spin-filtering capability ensures that different spin carriers travelling inside a given spin channel will

exit at different rates. In the ideal situation, the spin filter only allows one type of spins to cross the barrier and completely blocks the other type, allowing us to selectively probe spin information of this channel only. Here the spin orientation being probed is set by the magnetic orientation of the spin filter material. In most cases the exchange splitting moves the spin majority bands downward in energy (thus more filled) while moving the minority bands upward, and the detected spin orientation is therefore along the direction of "majority" spins within the barrier; certain materials could instead have one of their spin minority bands define the conduction band minimum, thus preferentially probe spins aligned along the minority channel - opposite to the barriers' magnetism direction. It is worth pointing out that the "majority" and "minority" here are relative to the magnetization direction of the spin filter, and the spin information to be probed does not have to be collinear with these two directions. If the desired spins are aligned at some angle with respect to the spin filter direction, the measurement is effectively taking the quantum projection of the spins in the selected direction.

Now that we have established that spin filters can be used as effective spin generators and spin analyzers, the simplest way to combine them together to verify these properties is to construct a vertical tunnel junction or a lateral spin valve consisting double spin filters [29,18]. The first spin filter serves as the spin polarizer, while the second one as the spin analyzer. Here we detail with the tunnel junction geometry to illustrate how this works. Its operation principle is shown in Fig.2. Let's first consider a conventional magnetic tunnel junction (MTJ) which consists of two ferromagnetic electrodes separated by a thin insulator tunnel barrier. The tunnel barrier can be treated as a simple energy barrier and the electrons cross this barrier through quantum mechanical tunneling. The tunnel conductance across this device is determined by the number of occupied electron states on the electrode for electrons to tunnel from, and the number

of empty states on the counter electrode for these electrons to tunnel into. In the absence of spin mixing events, one can readily find the total tunnel conductance of the device by adding up conductance from each spin channels. Understandably, the junction is in a low resistance state when the two spin reservoirs are aligned with each other and in a high resistance state when they are misaligned. The relative change of resistance is defined as the magnetoresistance (MR) ratio, and captured in the Julliere's model linking MR directly to spin polarization of the electrodes: $TMR = \frac{2P_1P_2}{1-P_1P_2}$; here P_1 and P_2 are the spin polarization of the two electrodes. A spin filter tunnel junction, on the other hand, does not involve magnetic electrodes. Instead, the spin transport is actively modulated inside a composite tunnel barrier consisting two spin filters. If the two spin filters are well aligned with each other, the majority electrons will face two low tunnel barriers and can cross the junction easily, leading to a low overall resistance on the device and a final transmission current dominated by the majority spins. If the two spin filters are misaligned, both spin channels will encounter one tall tunnel barrier and strongly attenuated, and the final junction resistance is therefore higher and the final transmission current is mixed with both types of carriers. We see that, in addition to creating a large resistance change on this spin filter tunnel junction, the same device is also able to turn on and off the spin polarization of the carriers flowing across it. Further analysis showed that the spin polarization can not only be turned on and off, but also varied, to a large extent linearly, to any desired values with bias voltages making it a true spin-valve, literally [30].

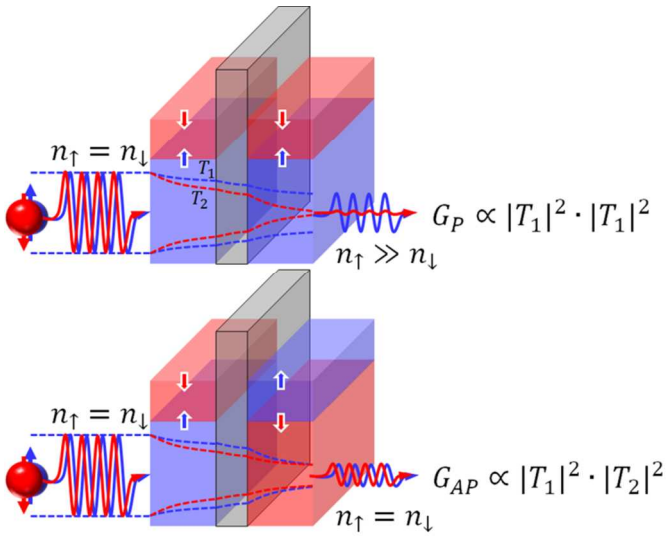

Fig.2 Illustration of a double spin filter tunnel junction, where a thin, regular insulator is inserted between the spin filters to magnetically decouple them. When the two spin filters are aligned parallel to each other, tunnel conductance is dominated by spin-up electrons; when they are aligned opposite to each other, the two spin channels have the same conductance and the final conductance equals twice the conductance of individual channels. Because $|T_1| \gg |T_2|$, we can easily see that the parallel conductance is much larger than the antiparallel conductance, leading to an appreciable magnetoresistance. In addition, we see that the parallel conductance is also highly spin-polarized while the antiparallel conductance is not. T_1 and T_2 are the transmission coefficients of the majority and minority electrons across a single spin filter barrier.

There are a number of important directions for the field of spin filtering. Inducing ferroelectric properties into spin filter materials makes it possible to create devices with four remnant memory states [31]: two from ferromagnetic switching, and two from ferroelectric switching (Fig.3), and potentially combines nonvolatile MRAM (magnetic random access memory) and FeRAM (ferroelectric random access memory) storage technologies together. The material that displays this property is $La_{0.1}Bi_{0.9}MnO_3$, which comes from a multiferroic (antiferromagnetic and ferroelectric) parent compound $BiMnO_3$, and doped with La for stabilizing ferromagnetism. Though its ferroelectric Curie temperature is well above room

temperature, its ferromagnetic Curie temperature is quite limited (90 K). Another promising multiferroic compound, Bi_2NiMnO_6, demonstrates somewhat stronger ferromagnetism and ferroelectricity, with the ferroelectric ordering temperature above room temperature yet the ferromagnetic ordering temperature still limited to 140K [32,33]. A possible way around this low ordering temperature problem is to use composite materials [34,35] - for example, coupling ferroelectric $BiFeO_3$ or $BaTiO_3$ with another ferromagnetic/ferrimagnetic material such as $CoFe_2O_4$ or $NiFe_2O_4$, to take advantage of both the ferroelectric and spin filter properties in these materials. There have been important works on nanocomposite of such systems [36,37,38,39,40], but epitaxial thin films of sufficient quality for device applications is yet to be fully developed [41,42].

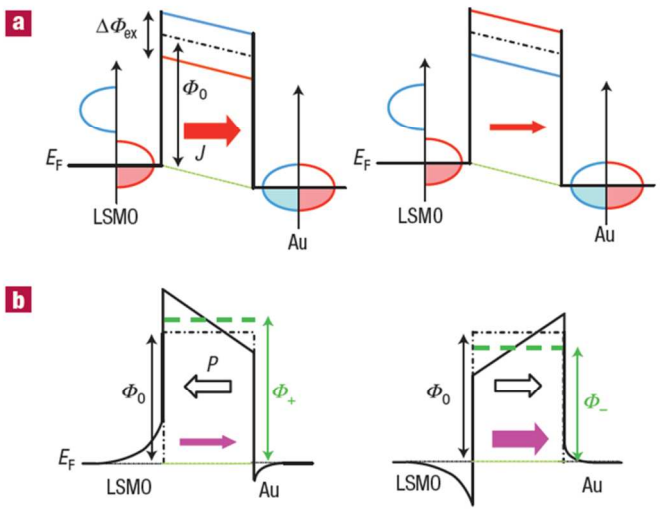

Fig.3 Illustration of the four-state device based on an $La_{0.67}Sr_{0.33}MnO_3/La_{0.1}Bi_{0.9}MnO_3$(2nm)/Au hybrid tunnel junction [31]. LSMO is a well-known half metal with nearly 100% spin polarization at the Fermi level, schematically illustrated with only a single band crossing E_F. (a) The high (left panel) and low (right panel) conductance states leading to magnetoresistance are established when the majority band of the ferromagnetic electrode (red band of LSMO) is aligned and antialigned with the majority band of the spin-filter (red barrier of LBMO), respectively; (b) The ferroelectric effect shows up as a voltage shift across the device depending on the electric polarization P inside the barrier, and can be set with previously applied electric fields (+/-1.5V across the

device). In both figures a) and b), the width of the filled red and magenta arrows schematically indicates the magnitude of the current flow in those configurations.

Spin filters make a natural choice for spin injection/detection across an extended conducting channel [43,44,45,46]. When a semiconductor channel is being considered, spin filters have a significant advantage in the sense that they are already semiconducting in nature, and less prone to the conductivity mismatch problem that restricts metallic injectors [44]. For example, when coupled to the organic semiconductors, such efficient spin injectors could potentially double the efficiency in spin OLEDs as well as generate spin-active devices such as organic spin valves and spin-OFETs [47,48,49,50,51]. The challenge in these directions however, is still the low Curie temperature associated with many of the materials of choice. Selected doping on some materials can raise the Curie temperature to some extent, for example, C doping on GdN can potentially raise its T_C from 70 K up to 190 K [52], and La and Gd doping on EuO were shown to raise its T_C from 69 K to 200 K [53] and 170 K [54], respectively. The magnetic nature of these materials also enables modulation of supercurrent phases across these barriers, and makes it possible to vary the barrier thickness to create Josephson junctions with non-zero ground state Josephson phases (Fig.4), for example, π-junctions [55,56,57] that are proposed for achieving coherent superconducting qubits without an external field and for realizing long range spin polarized transport with dissipationless supercurrents.

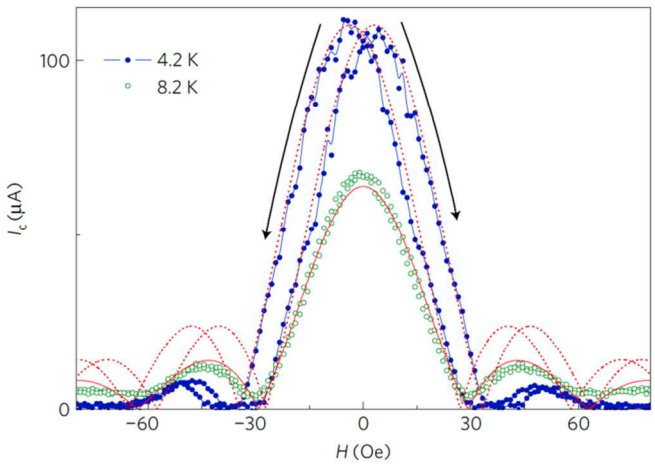

Fig.4 Critical current Fraunhofer pattern of NbN–GdN–NbN junction [56]. The clear hysteresis behavior with field sweep direction (arrows) indicates that the internal magnetization from GdN barrier modifies the total flux enclosed by the Josephson junction. The maximum critical current is suppressed with increasing spin filter efficiency due to blocking on one of the spin channels.

II. Interfacial exchange Zeeman field

A magnetic semiconductor naturally contains a large number of localized magnetic moments. In the following discussions, we will ignore the magnetic moments from electrons' orbital motion because those components do not contribute to the exchange fields we are interested in. In most systems, the magnetic moments are generated by electron spins, especially from electrons occupying the spatially localized *d* and *f* orbitals. The commonly encountered magnetic materials often involve 3*d* transition elements and/or 4*f* rare-earth elements. Electrons being Fermions, must have antisymmetric wavefunctions among themselves. The net consequence is that the combined spatial wave function of any two electrons is dependent on the relative spin configuration of these electrons (i.e., the spin singlet and triplet states). The different electron spatial distribution will lead to difference in the system's energy, such as the Coulomb energy and kinetic energy, thus renders one of the spin states with lower energy than

the other one. Such an energy splitting is known as the exchange energy. As a result, a system can collectively exhibit macroscopical ferromagnetic, antiferromagnetic, and many other magnetic configurations. The exchange interaction can be generalized to between two neighboring magnetic ions, which is essentially sum of contributions from every pair of electrons. In the Heisenberg model, the exchange energy can be written as $\mathcal{H} = -2J_e S_1 \cdot S_2$, where J_e is the exchange energy constant, and $\boldsymbol{S}_1$, $\boldsymbol{S}_2$ are the spins of the two magnetic ions. The exchange energy constant can be readily deduced from the exchange stiffness of the material. For example, J_e is around 12 meV for body-centered-cubic Fe, and about 13 meV for face-centered-cubic Ni [58]. The exchange energy constants, together with the number of exchange neighbors, determine the Curie temperature in these materials.

The above described scenario assumes that electrons have direct wavefunction overlap. If the two electrons are spatially separated with negligible wavefunction overlap, being in the singlet state or triplet state will not change the system energy and no exchange interaction should be expected. It is however possible for them to interact through a common intermediate state and experience a mutual "indirect" exchange interaction [59] commonly referred as Vonsovsky-Zener exchange model [60,61]. It is in some sense the metallic analogue of superexchange in insulators. For an itinerant ferromagnet such as Fe, the localized 3*d* electrons exchange with, and induce spin polarization into, the *sp* conduction electrons, which then proceed to exchange with the adjacent 3*d* electrons and align them ferromagnetically. In this case, the indirect exchange interaction is mediated through the conduction electrons and the strength follows Ruderman-Kittel-Kasuya-Yosida (RKKY) oscillation [62] with interatomic spacing. For magnetic materials involving rare-earth elements, the magnetic 4*f* electrons are deeply buried under the 5*s* and 5*p* shells, thus direct exchange is negligibly small and indirect exchange dominates in these systems.

The strength of the exchange interaction between conduction electrons and rare-earth compounds is of a similar order of magnitude around 10 meV [63,64].

For a magnetic semiconductor involving localized *d* or *f* electrons, the same indirect exchange interaction mechanism can propagate into the adjacent metals, polarizing their conduction electrons. This is equivalent to inducing a Zeeman field onto that bordering free electron system. Because the exchange interaction initiates from the interface between the magnetic semiconductor and the metal, one can expect that the overall effective Zeeman field decays rapidly with the thickness of the metal layer. For thin electronic systems, such as a thin metal film or a 2D electron gas, the film thickness is far below the electrons' mean free path and all electrons in the layer have the same probability to interact through the interface with the magnetic semiconductor. As a result, the effective Zeeman field strength is "diluted" by the total number of carriers on the metal side and shows overall 1/*d* dependence with respect to the film thickness *d*. The additional RKKY oscillation roughly follows $\frac{\sin(2k_F d)}{d^2}$ dependence with *d*, here k_F is the Fermi wave vector of the electrons within the metal. Due to the very fast oscillation of this function, after the first few Ångströms, the averaged exchange strength over all the electrons still follows approximately 1/*d* dependence. Experimentally, a 1/*d* dependence of the induced Zeeman field was indeed reported on thin Al films in contact with EuO [65].

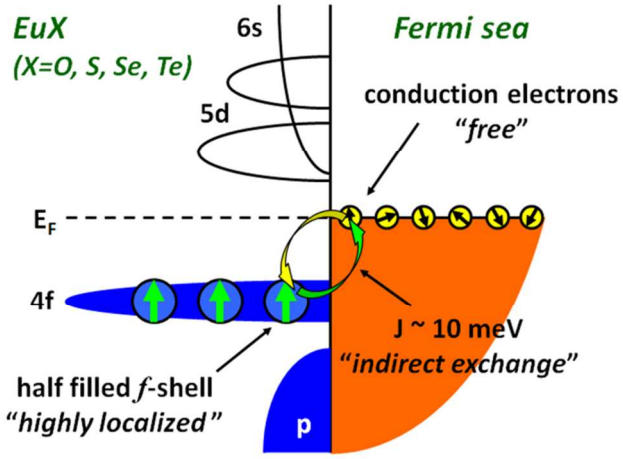

Fig.5 Illustration of the indirect exchange interaction between conduction electrons and the localized 4f electrons of Europium chalcogenide compounds. The exchange constant was determined to be around 10 meV [63,64] on these systems, and the coupling antiferromagnetic [7,66].

There are a number of unique experiments in the literature to take advantage of the strong exchange field coupled with superconductor systems. The previously mentioned Meservey-Tedrow technique [5], a standard way of probing spin polarization of a tunnel current, was successfully employed on Au/EuS/Al tunnel junctions without applying an external magnetic field **[7].** Well-resolved spin splitting appears due to the strong internal exchange field from EuS spin filter barrier. And for the thin Al films, the proximity induced internal field behaves no different from an external applied (Zeeman) field, but it is now a local parameter easily tunable with magnetic configuration of the spin filter films. One can, for example, vary the relative orientation of two spin filter layer to enhance or cancel the combined internal fields, resulting in tunable superconductivity in EuS/Al/EuS superconducting spin valves (Fig.6) [67]. In a mesoscopic structure containing superconductor Al channel with EuS in proximity, the induced exchange field on the superconductor quasi particles modifies the spin polarized transport in the channel, making it an additional control parameter for spin current flow in superconductors [46].

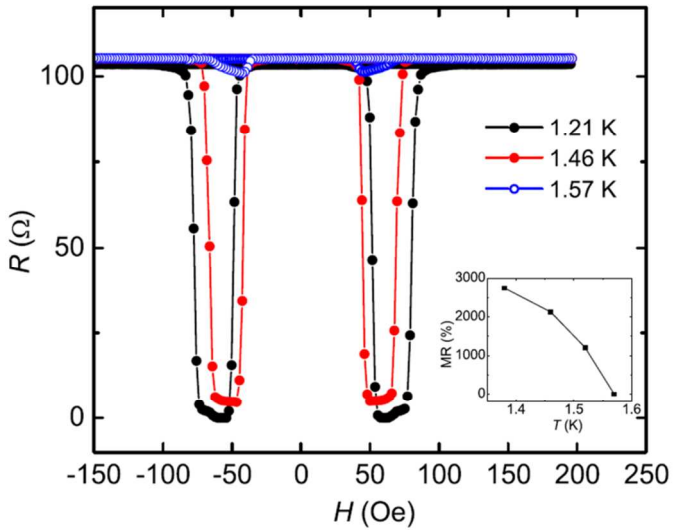

Fig.6 A superconducting spin switch driven by strong internal exchange fields [67]. The device is based on a sandwich structure of EuS(1.5nm)/Al(3.5nm)/EuS(4nm). As superconductivity is relatively weak near T_C, the exchange fields from the magnetic semiconductors become strong enough to turn the superconductivity on and off: the system is in a superconductivity-off state (R~100Ω) when the two EuS layers are aligned with each other strengthening the exchange fields; and returns to the superconductivity-on state (R~0Ω) when the two EuS layers are antialigned and exchange fields canceled. Inset shows the temperature dependence of this effect.

We next use a simple model as detailed by Haugen *et al* [68] to estimate the order of magnitude on the strength of this effective Zeeman field. For a system with a rare-earth based magnetic semiconductor EuO on top of a 2DEG graphene, the effective Zeeman field is estimated to be about 5 meV, or equivalent to a field strength of 80 T. The effect is most dramatic for 2D electronic system where the carrier density is low and magnetic proximity is strong. Such strong exchange field has been optically confirmed on EuS-coated single-walled carbon nanotubes by looking at photocurrent signatures from the triplet excitons, where the exchange field functions as a mixing mechanism for the singlet and triplet channels to enable optical activity [69]. In addition, this interfacial "field" can be readily manipulated with a much smaller external magnetic field (≈10mT for in-plane switching and ≈1T for out-of-plane

switching) by rotating the macroscopical magnetization of the EuO film. Due to the electron-electron exchange nature of this interfacial field, the resultant effective Zeeman field only applies to the electron gas's spin degree of freedom, not on its orbital degree of freedom. For example, despite the effective Zeeman field being routinely larger than tens of Tesla, one cannot expect to observe Quantum Hall Effect from this field alone because there would be no Landau levels forming. When coupled to 2D electronic systems such as graphene and silicene, strong perpendicular exchange field breaks time-reversal symmetry and appreciable Rashba spin-orbit interaction develops at the interface due to structural inversion asymmetry, and together they can induce quantum anomalous Hall effect [70] in these systems [71,72]. Lately there has been some important progress on proximity induced exchange fields onto surface states of topological insulators [73]. A closely related experiment [74] has been realized recently in $Cr_{0.15}(Bi_{0.1}Sb_{0.9})_{1.85}Te_3$, a magnetically doped 3D topological insulator, where the exchange field comes from dopants in the bulk rather than from proximity across interfaces.

Because one can use a small applied magnetic field to induce a giant Zeeman field which would otherwise be formidable for a normal laboratory, such an interfacial field is of great value for designing novel spintronic devices. It can lift the degeneracy of a spin system and make different spin states readily distinguishable. There are some elegant theoretical proposals yet to be fully carried out experimentally. For example, one can use a heterostructure consisting of a semiconductor sandwiched between a magnetic semiconductor and an s-wave superconductor, to induce both magnetic and superconducting proximity onto the conduction band of the semiconductor [75]. The Rashba split bands closely mimic the Dirac bands of a topological insulator surface, which, when coupled to an *s*-wave superconductor through proximity, is known to support formation of Majorana bound states at vortices core or other boundaries [76].

A critical difference is that this semiconductor platform is spin degenerate, which prevents the desired non-Abelian statistics from appearing. Therefore a strong perpendicular exchange field (or a real magnetic field of enough strength) is necessary to open up an energy gap at the "Dirac" point and leaves only one band crossing the Fermi surface - ready for hosting non-Abelian topological order when an s-wave superconductor is also introduced (Fig.7). With all the ingredients in place, Majorana fermions emerge inside superconductor vortices and can be braided as if they are actual particles. Similarly, pairs of Majoranas also nucleate on the ends of 1D nanowires of semiconductors or metals, in the presence of strong Rashba spin-orbit coupling, superconducting proximity effect and Zeeman splitting, as theoretically predicted [77,78,79,80] and experimentally demonstrated by many groups [81,82,83,84,85]. The special non-Abelian nature of these particles makes it possible to construct topological quantum computers [86,87] which are inherently fault-tolerant to a very high threshold [88,89].

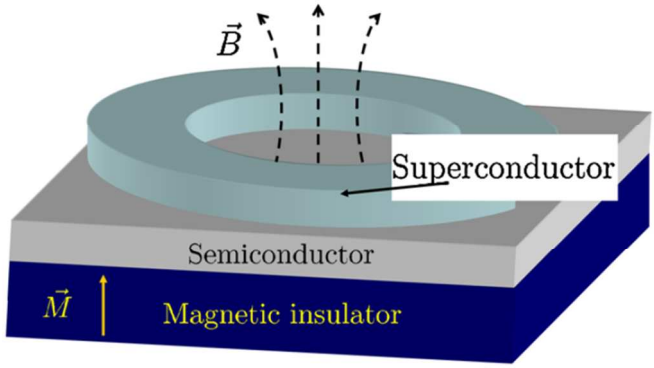

Fig.7 A proposed semiconductor heterostructure with both superconducting and magnetic proximity and can host the existence of a Majorana bound state inside a vortex core [75].

III. Spin Regulation

With the unique properties of spin filter tunnel barriers, it becomes possible to create a composite structure for shuffling spins in desired directions in order to achieve spin regulation

[90]. This was achieved by individually creating an asymmetric spin barrier profile for each spin channel, and excited spins exit the device with asymmetric probabilities in a motion similar to the unidirectional AC-to-DC rectification from a diode, except that the two spin channels are regulated towards opposite directions. To convert the pure spin information to a detectable voltage signal, the intrinsic interfacial exchange field as described in the previous section serves as the necessary ingredient to render the chemical potentials of the two spin channels different from each other.

The basic structure consists of a double spin-filter tunnel junction of two EuS spin filter barriers with small metallic Al nano-islands sandwiched in between, as illustrated in Fig.8. EuS has bulk Curie temperature of 16.6 K and creates interfacial Zeeman field on the order of several Tesla for thin Al films of a few nm [8]. For even thinner Al films, the effective field goes up quickly, inverse to the film thickness as detailed in the previous section. The direction of the interfacial field in this system is determined to be opposite to the magnetization of the spin filter material, consistent with literature reports from transport and NMR measurements [7,66]. The strong Zeeman splitting ensures that electrons confined on the nano-islands and with minority spins would occupy energy levels uniformly lower than their majority-spin counterparts. For a single electron trapped on a Coulomb island, it can occupy one of the two exchange-split states; provided that the external fluctuation energy is strong enough, the two states would have essentially equal population. For the islands with double occupancy, due to Pauli principle, the two electrons can only settle in with opposite spins, and the next available excitation level is well isolated by the Coulomb charging energy. In this system, the interface-induced Zeeman splitting is much smaller than the Coulomb charging energy. Therefore mild fluctuations in the system, for example, from electronic noise and thermal fluctuations, can readily saturate the spin states of

the single occupancy islands, but can hardly trigger any excitations on the double occupancy islands. The intrinsic on-dot spin lifetime is expected to be very long due to weak spin-orbit coupling of Al and spatial confinement of these quantum dots, and spin relaxation mainly happens through electron tunnel communication with the electrodes.

If the spin filters are ideal, they will only permit one type of spins to communicate through these barriers, and the spin channel parallel to the spin filter barrier tends to have its chemical potential aligned through the barrier with the electrode. The spin splitting on the nano-islands will therefore pass onto the electrodes, and create a measureable voltage signal across the device. Naturally, such a voltage signal is only achievable when the two spin filters are placed in the antiparallel configuration, and spin-up electrons flow one way while spin-down ones the opposite way. The internal spin splitting on the nano-islands renders different chemical potentials for the electrons heading opposite ways, while external perturbations ensure the two spin levels are sufficiently populated which also supplies energy to the process. When the two spin filters are aligned parallel to each other, however, the device is spin symmetric and no spin signal development is possible. Therefore with sweeping magnetic fields, a voltage signal develops across the device in the antiparallel state and vanishes in the parallel state. In practice, spin filters are not ideal and the “forbidden” spin channel can still participate in the communication, and bring down the observable spin signal. The actual detected signal corresponds to the internal exchange splitting modulated by the spin filtering efficiency of the barriers, which is roughly 40% for EuS based structures.

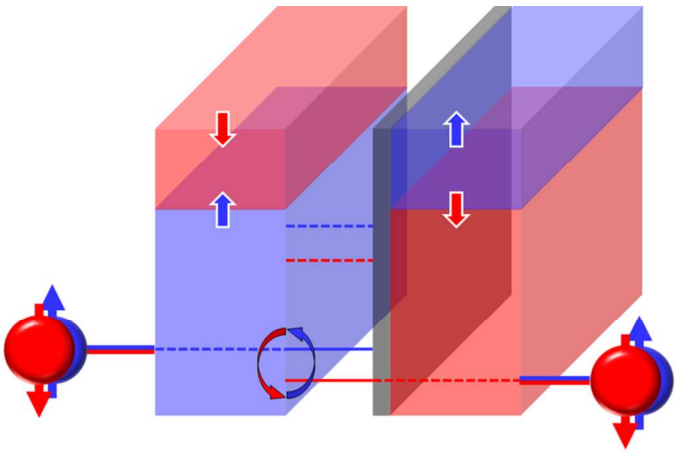

Fig.8 Illustration of a double spin filter device with Zeeman split levels in between. When the two relevant levels are sufficiently populated, a voltage response will develop across the device because only one type of spins can flow through each barrier. On this schematic, the middle Coulomb island sees interfacial exchange interaction only on its left side interface; its right side forms an opaque barrier to stop exchange interactions from this side.

In addition to the spontaneous spin flow as shown above, the fact that spins only travel in predefined direction allows one to design active spin regulation devices. We have touched on this in Section I, and that in addition to showing magnetoresistance, a double spin filter tunnel junction can also modify the spin polarization of the transient current (Fig.2). The net spin polarization is nearly 100% when the two spin filters are aligned, and zero when they are antialigned. The spin polarization in the antialigned configuration is no longer zero under finite bias voltages: it varies almost linearly with the bias voltage [30], allowing one to not only turn the spin polarization on and off, but also set it continuously to any finite value desired.

When coupled with superconductors, the strong exchange fields from magnetic semiconductors make it possible to create large thermoelectric effect in the superconductors which lacks thermoelectric response on their own. The dual functionalities of the magnetic semiconductors are cleverly explored in a superconductor/magnetic semiconductor/normal metal

system [91]: interfacial exchange fields to remove the electron-hole symmetry on individual spin channels, while spin filter tunneling to select the desired spin channel only. This configuration offers thermoelectric efficiency much larger than conventional materials and approaching the Carnot limit. The device's thermoelectric properties become readily flux tunable when coupled to the weak link of a SQUID, making it possible to perform effective thermal management in the superconductor systems.

On the quantum frontiers, it is possible to construct a spin detector at a single electron level. One can use a spin filter barrier to perform one-shot readout on a single electron spin through charge sensing – a "swap gate" operation on the charge and spin quantum states (Fig.9) [92]. When a single electron wavefunction is ready for readout, one can apply a gate voltage to press this wavefunction against a spin filter barrier, and the spin detection is now converted into a charge detection: we know the spin is aligned with the spin filter direction if the electron's wavefunction readily extends across the barrier, and the spin is opposite to the spin filter direction if the wavefunction mostly stays confined. When the interfacial exchange field is also in action, this spin-qubit receives a natural splitting on the two levels, but may also experience additional decoherence due to the spatially inhomogeneous exchange field.

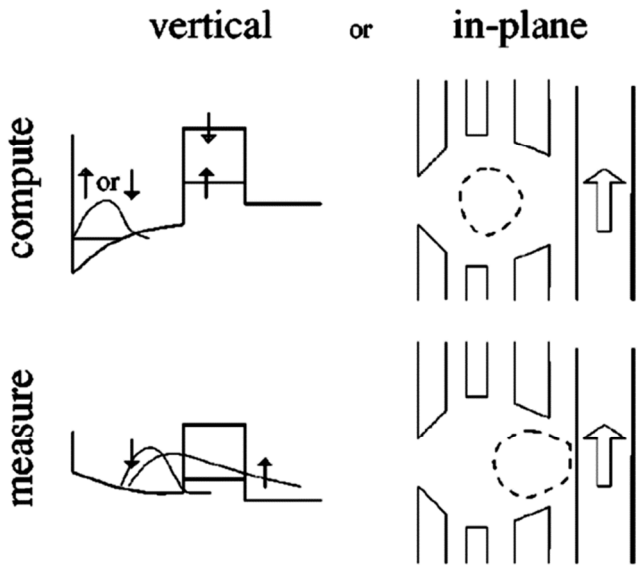

Fig.9 Illustration of the proposed single spin readout with spin filters, possible vertical and in-plane structures are shown [92]. The electron is kept far away from the spin filter when quantum computing is in progress. When the spin information is ready for readout, a gate voltage is applied which presses the electron wavefunction against the spin filter. Whether or not one can find the electron's wavefunction on the other side of the spin filter barrier is directly determined by the spin orientation of the wavefunction. Position of an electron is readily measurable with capacitive charge sensing.

IV. Summary

From the above examples, we see that we can use magnetic semiconductors as functional barriers, which can be subsequently tuned with external magnetic fields to generate the desired energy profiles for individual spin channels. Each of these barriers is a spin selective component suitable for providing spin regulations. These spin filters do not have to be configured collinear in directions, and each filtering stage is effectively taking a projection measurement along the newly defined principle axis. By controlling the spin filter material's properties and device geometries, one can induce different magnetic anisotropies in them and enable individual control through external fields. A magnetic semiconductor also generates an extremely strong interfacial

exchange field on the adjacent electron gases, and a small applied field can efficiently induce and rotate the much larger exchange Zeeman field with strength exceeding tens of Tesla. This effective field is most effective on low dimensional electronic systems and capable of lifting the degeneracy of electron spins or other composite particles formed from correlated electrons. In addition to these passive properties, active spin regulation is readily achievable when one dynamically tunes the magnetic energy profiles of the two spin channels, via external controls with applied magnetic field and gate electric field operations. With these additional control parameters one can valve the spins to flow in desired directions.

So far, we focus on the transport phenomena involving magnetic semiconductors but only in the ballistic, short distance tunneling and proximity regime. Magnetic semiconductors, when conductive enough, can also become an effective spin transport media in the diffusive, long distance carrier hopping regime. Such processes have been demonstrated in a large variety of dilute magnetic semiconductor (DMS) materials, such as magnetically doped II-VI, III-V, and oxide semiconductors [93,94,95,96]. Dilute magnetic semiconductors are often based on nonmagnetic host materials, and then heavily doped into showing ferromagnetic behavior. Therefore they tend to structurally well match conventional semiconductors and ready for device integration. While many of the III-V and II-VI based dilute magnetic semiconductors still suffer from lower than room temperature Curie temperatures, some of the oxide based dilute magnetic semiconductor materials have already shown performance at much higher than room temperature [96]. Spins have extremely long lifetime and coherence length in these materials and the spin information is also optically maneuverable and detectable. Carriers gain their spin polarization through interaction with localized dopants, which in turn order them ferromagnetically. Spins are therefore constantly being polarized in their conduction channels rather than filtered by selective

quantum tunneling, and an interfacial exchange field, weaker due to the dilute presence of localized moments, can also propagate across the interface into the adjacent electron systems. These are the main difference between the dilute magnetic semiconductors and the previously described intrinsic magnetic semiconductors. Topics involving dilute magnetic semiconductors have been extensively reviewed in the literature [97,98,99,96,100] therefore we will not cover it any more in this article.

Overall, the basic properties of magnetic semiconductors are quite well understood by now, and the major challenge in the field lies in the development of suitable materials. This includes developing materials with higher Curie temperature for room temperature operations, and materials with fewer defects for improved efficiencies. For example, we see that the experimentally determined spin filter efficiency in ferrites is no more than 40% in actual devices, and barely a few percent remains at room temperature, far less than theoretically expected. Eliminating undesired structural and compositional defects from the materials will reveal the full potential of spin filters. The inherent interfacial exchange fields from localized moments are not prone to the material imperfections, but are sensitive to the interfacial configuration. For example, an ordered interface can generate periodic spin potentials on the atomic scale, which could yield rich physics when imposed on top of other periodic electronic structures [101,102]. Such experiments call for atomically sharp interface and strict structural correlation, again require extensive atomic level materials engineering. We expect that with further refinement on materials systems will bring the field fast forward and open vast possibilities for spintronics applications.

Acknowledgement: This research is supported by the grants NSF (DMR-1207469), ONR (N00014-13-1-0301), and NSERC DISCOVERY (RGPIN 418415-2012).

[1] L. Esaki, P.J. Stiles, S. von Molnar, Magnetointernal Field Emission in Junctions of Magnetic Insulators, Phys. Rev. Lett. **19**, 852 (1967).

[2] N. Müller, W. Eckstein, W. Heiland, W. Zinn, Electron Spin Polarization in Field Emission from EuS-Coated Tungsten Tips, Phys. Rev. Lett. **29**, 1651 (1972).

[3] J. S. Moodera, T. S. Santos and T. Nagahama, The phenomena of spin filter tunneling, J. Phys.: Condens. Matter 19, 165202 (2007).

[4] J.S. Moodera, G.X. Miao, T.S. Santos, Frontiers in Spin Polarized Tunneling, Physics Today 63, 46 (2010).

[5] R. Meservey, P.M. Tedrow, Spin-polarized electron tunneling, Physics Reports **238**, 173–243 (1994).

[6] T.S. Santos and J.S. Moodera, Observation of Spin-Filtering with Ferromagnetic Europium Monoxide Tunnel Barrier, Phys. Rev. B **69**, 241203(R) (2004).

[7] J. S. Moodera, X. Hao, G. A. Gibson, R. Meservey, Electron-Spin Polarization in Tunnel Junctions in Zero Applied Field with Ferromagnetic EuS Barriers, Phys. Rev. Lett. 61, 637 (1988).

[8] X. Hao, J. S. Moodera, R. Meservey, Spin-filter effect of ferromagnetic europium sulfide tunnel barriers, Phys. Rev. B 42, 8235 (1990).

[9] A.V. Ramos, T.S. Santos, G.X. Miao, M.J. Guittet, J.B. Moussy, J.S. Moodera, Influence of oxidation on the spin-filtering properties of $CoFe_2O_4$ and the resultant spin polarization, Phys. Rev. B 78, 180402(R) (2008).

[10] S. Matzen, J.B. Moussy, G.X. Miao, J.S. Moodera, Direct evidence of spin filtering across $MnFe_2O_4$ tunnel barrier by Meservey-Tedrow experiment, Phys. Rev. B 87, 184422 (2013).

[11] R.J. Soulen Jr., J.M. Byers, M.S. Osofsky, B. Nadgorny, T. Ambrose, S.F. Cheng, P.R. Broussard, C.T. Tanaka, J. Nowak, J.S. Moodera, A. Barry, J.M.D. Coey, Measuring the Spin Polarization of a Metal with a Superconducting Point Contact, Science 282, 85 (1998).

[12] F. Rigato, S. Piano, M. Foerster, F. Giubileo, A.M. Cucolo, J. Fontcuberta, Direct determination of the spin filter efficiency in ferrimagnetic $CoFe_2O_4/SrRuO_3$ tunnel junctions by Andreev reflection, Phys. Rev. B 81, 174415 (2010).

[13] T.S. Santos, J.S. Moodera, K.V. Raman, E. Negusse, J. Holroyd, J. Dvorak, M. Liberati, Y.U. Idzerda, E. Arenholz, Determining Exchange Splitting in a Magnetic Semiconductor by Spin-Filter Tunneling, Phys. Rev. Lett. **101**, 147201 (2008).

[14] A. Pal, K. Senapati, Z.H. Barber, M.G. Blamire, Electric-Field-Dependent Spin Polarization in GdN Spin Filter Tunnel Junctions, Adv. Mater. **25**, 5581–5585 (2013).

[15] B. Prasad, M. Egilmez, F. Schoofs, T. Fix, M.E. Vickers, W. Zhang, J. Jian, H. Wang, M.G. Blamire, Nanopillar Spin Filter Tunnel Junctions with Manganite Barriers, Nano Lett. 14, 2789 (2014).

[16] P. LeClair, J.K. Ha, H.J.M. Swagten, J.T. Kohlhepp, C.H. van de Vin, W.J.M. de Jonge, Large magnetoresistance using hybrid spin filter devices, Appl. Phys. Lett. 80, 625 (2002).

[17] T. Nagahama, T.S. Santos, J.S. Moodera, Enhanced magneto-transport at high bias in quasi-magnetic tunnel junctions with EuS spin-filter barriers , *Phys. Rev. Lett.* **99**, 016602 (2007).

[18] G.X. Miao, M. Müller, J.S. Moodera, Magnetoresistance in Double Spin Filter Tunnel Junctions with Nonmagnetic Electrodes and its Unconventional Bias Dependence, Phys. Rev. Lett. **102**, 076601 (2009).

[19] G.X. Miao, J.S. Moodera, Magnetic tunnel junctions with MgO-EuO composite tunnel barriers, Phys. Rev. B **85**, 144424 (2012).

[20] U. Lüders, M. Bibes, K. Bouzehouane, E. Jacquet, J.P. Contour, S. Fusil, J.F. Bobo, J. Fontcuberta, A. Barthélémy, A. Fert, Spin filtering through ferrimagnetic $NiFe_2O_4$ tunnel barriers, Appl. Phys. Lett. 88, 082505 (2006).

[21] M. Gajek, M. Bibes, A. Barthélémy, K. Bouzehouane, S. Fusil, M. Varela, J. Fontcuberta, A. Fert, Spin filtering through ferromagnetic BiMnO3 tunnel barriers, Phys. Rev. B 72, 020406(R) (2005).

[22] T. Harada, I. Ohkubo, M. Lippmaa, Y. Sakurai, Y. Matsumoto, S. Muto, H. Koinuma, M. Oshima, Spin-Filter Tunnel Junction with Matched Fermi Surfaces, Phys. Rev. Lett. 109, 076602 (2012).

[23] A.V. Ramos, M.J. Guittet, J.B. Moussy, R. Mattana, C. Deranlot, F. Petroff, C. Gatel, Room temperature spin filtering in epitaxial cobalt-ferrite tunnel barriers, Appl. Phys. Lett. 91, 122107 (2007).

[24] Y.K. Takahashi, S. Kasai, T. Furubayashi, S. Mitani, K. Inomata1, K. Hono, High spin-filter efficiency in a Co ferrite fabricated by a thermal oxidation, Appl. Phys. Lett. 96, 072512 (2010).

[25] S. Matzen, J.B. Moussy, R. Mattana, K. Bouzehouane, C. Deranlot, F. Petroff, Appl. Phys. Lett. 101, 042409 (2012).

[26] Z. Szotek, W.M. Temmerman, D. Koedderitzsch, A. Svane, L. Petit, H. Winter, Electronic structure of normal and inverse spinel ferrites from first principles, Phys. Rev. B 74, 174431 (2006).

[27] N.M. Caffrey, D. Fritsch, T. Archer, S. Sanvito, C. Ederer, Spin-filtering efficiency of ferrimagnetic spinels CoFe2O4 and NiFe2O4, Phys. Rev. B 87, 024419 (2013).

[28] M.G. Chapline, S.X. Wang, Room-temperature spin filtering in a $CoFe_2O_4/MgAl_2O_4/Fe_3O_4$ magnetic tunnel barrier, Phys. Rev. B 74, 014418 (2006).

[29] D.C. Worledge, T.H. Geballe, Magnetoresistive double spin filter tunnel junction, J. Appl. Phys. **88**, 5277 (2000).

[30] G.X. Miao, J.S. Moodera, Spin switch based on double spin-filter tunnel junction geometry, J. Appl. Phys. 108, 083910 (2010).

[31] M. Gajek, M. Bibes, S. Fusil, K. Bouzehouane, J. Fontcuberta, A. Barthélémy, A. Fert, Tunnel junctions with multiferroic barriers, Nat. Mater. 4, 296-302 (2007).

[32] M. Azuma, K. Takata, T. Saito, S. Ishiwata, Y. Shimakawa, M. Takano, Designed Ferromagnetic, Ferroelectric Bi2NiMnO6, J. Am. Chem. Soc. 127, 8889 (2005).

[33] M. Sakai, A. Masuno, D. Kan, M. Hashisaka, K. Takata, M. Azuma, M. Takano, Y. Shimakawa, Multiferroic thin film of Bi2NiMnO6 with ordered double-perovskite structure, Appl. Phys. Lett. 90, 072903 (2007).

[34] R. Ramesh, N.A. Spaldin, Multiferroics: progress and prospects in thin films, Nature Materials 6, 21-29 (2007).

[35] Y. Shimakawa, M. Azuma, N. Ichikawa, Multiferroic Compounds with Double-Perovskite Structures, Materials 4, 153-168 (2011).

[36] K. Ueda, H. Tabata, T. Kawai, Coexistence of ferroelectricity and ferromagnetism in $BiFeO_3$–$BaTiO_3$ thin films at room temperature, Appl. Phys. Lett. 75, 555 (1999).

[37] F. Zavaliche, H. Zheng, L. Mohaddes-Ardabili, S.Y. Yang, Q. Zhan, P. Shafer, E. Reilly, R. Chopdekar, Y. Jia, P. Wright, D.G. Schlom, Y. Suzuki, R. Ramesh, Electric Field-Induced Magnetization Switching in Epitaxial Columnar Nanostructures, Nano Lett. 5, 1793 (2005).

[38] H. Zheng, F. Straub, Q. Zhan, P.L. Yang, W.K. Hsieh, F. Zavaliche, Y.H. Chu, U. Dahmen, R. Ramesh, Self-Assembled Growth of $BiFeO_3$–$CoFe_2O_4$ Nanostructures, Adv. Mater. 18, 2747 (2006).

[39] J.L. Ma Cmanus-Driscoll, P. Zerrer, H.Y. Wang, H. Yang, J. Yoon, A. Fouchet, R. Yu, M.G. Blamire, Q.X. Jia, Strain control and spontaneous phase ordering in vertical nanocomposite heteroepitaxial thin films, Nat. Mater. 7, 314 (2008).

[40] D.H Kim, N.M. Aimon, X.Y. Sun, L. Kornblum, F.J. Walker, C.H. Ahn, C.A. Ross, Integration of Self-Assembled Epitaxial $BiFeO_3$–$CoFe_2O_4$ Multiferroic Nanocomposites on Silicon Substrates, Adv. Funct. Mater. 24, 33 (2014).

[41] H. Toupet, V.V. Shvartsman, F. LeMarrec, P. Borisov, W. Kleemann, M. Karkut, Enhanced Magnetization in $BiFeO_3/BaTiO_3$ Multilayers, Integr. Ferroelectr. 100, 165 (2008).

[42] Z.G. Wang, Y.D. Yang, R. Viswan, J.F. Li, D. Viehland, Giant electric field controlled magnetic anisotropy in epitaxial $BiFeO_3$-$CoFe_2O_4$ thin film heterostructures on single crystal $Pb(Mg_{1/3}Nb_{2/3})_{(0.7)}Ti_{0.3}O_3$ substrate, Appl. Phys. Lett. 99, 043110 (2011).

[43] R. Fiederling, M. Keim, G. Reuscher, W. Ossau, G. Schmidt, A. Waag, L. W. Molenkamp, Injection and detection of a spin-polarized current in a light-emitting diode, Nature **402**, 787-790 (1999).

[44] G Schmidt, Concepts for spin injection into semiconductors - a review, J. Phys. D: Appl. Phys. 38, R107 (2005).

[45] M. Müller, M. Luysberg, C.M. Schneider, Observation of spin filtering in magnetic insulator contacts to silicon, Appl. Phys. Lett. 98, 142503 (2011).

[46] M.J. Wolf, C. Sürgers, G. Fischer, D. Beckmann, Spin-polarized quasiparticle transport in exchange-split superconducting aluminum on europium sulfide, Phys. Rev. B 90, 144509 (2014).

[47] T.D. Nguyen, E. Ehrenfreund, Z.V. Vardeny, Spin-Polarized Light-Emitting Diode Based on an Organic Bipolar Spin Valve, Science 337(6091), 204-209 (2012).

[48] C. Boehme, J.M. Lupton, Challenges for organic spintronics, Nature Nanotechnology 8, 612–615 (2013).

[49] B. Minaev, G. Baryshnikovb, H. Agrena, Principles of phosphorescent organic light emitting devices, Phys. Chem. Chem. Phys.16, 1719-1758 (2014).

[50] K. V. Raman, A. M. Kamerbeek, N. Atodiresei, A. Mukherjee, T. K. Sen, P. Lazić, V. Caciuc, R. Michel, D. Stalke, S. K. Mandal, S. Blügel, M. Münzenberg, J. S. Moodera, Interface engineered templates for molecular spin memory and sensor devices, Nature, 493, 509-513 (2013)

[51] D. Sun, E. Ehrenfreund, Z.V. Vardeny, The first decade of organic spintronics research, Chem. Commun. 50, 1781-1793 (2014).

[52] M. Kuznietz, Effect of Substitutional Anions on the Magnetic Properties of the Mononitrides of Uranium and Gadolinium, J. Appl. Phys. 42, 1470 (1971).

[53] H. Miyazaki, H.J. Im, K. Terashima, S. Yagi, M. Kato, K. Soda, T. Ito, S. Kimura, La-doped EuO: A rare earth ferromagnetic semiconductor with the highest Curie temperature, Appl. Phys. Lett. 96, 232503 (2010).

[54] H. Ott, S.J. Heise, R. Sutarto, Z. Hu, C.F. Chang, H.H. Hsieh, H.J. Lin, C.T. Chen, L.H. Tjeng, Soft x-ray magnetic circular dichroism study on Gd-doped EuO thin films, Phys. Rev. B 73, 094407 (2006).

[55] T. Yamashita, K. Tanikawa, S. Takahashi, S. Maekawa, Superconducting π Qubit with a Ferromagnetic Josephson Junction, Phys. Rev. Lett. 95, 097001 (2005).

[56] K. Senapati, M.G. Blamire, Z.H. Barber, Spin-filter Josephson junctions, Nat. Mater. 10, 849 (2011).

[57] F.S. Bergeret, A. Verso, A.F. Volkov, Electronic transport through ferromagnetic and superconducting junctions with spin-filter tunneling barriers, Phys. Rev. B 86, 214516 (2012).

[58] A.H. Morrish, The physical principles of magnetism, John Wiley & Son Inc. (1965).

[59] A. Mauger, Indirect Exchange in Europium Chalcogenides, Phys. Stat. Sol. B 84, 761 (1977).

[60] S.V. Vonsovsky, On the exchange interaction of s and d electrons in ferromagnets, Zh. Eksp. Teor. Fiz. 16, 981 (1946).

[61] C. Zener, Interaction between the d shells in the transition metals, Phys. Rev. 81, 440 (1951).

[62] M.A. Ruderman, C. Kittel, Indirect Exchange Coupling of Nuclear Magnetic Moments by Conduction Electrons, Phys. Rev. 96, 99 (1954); T. Kasuya, A Theory of Metallic Ferro- and Antiferromagnetism on Zener's Model, Prog. Theor. Phys. 16, 45 (1956); K. Yosida, Magnetic Properties of Cu-Mn Alloys, Phys. Rev. 106, 893 (1957).

[63] J.E. Tkaczyk, P.M. Tedrow, Magnetic proximity effect at a superconductor-rare-earth oxide interface, J. Appl. Phys. 61, 3368 (1987).

[64] G.M. Roesler, Jr., M.E. Filipkowski, P.R. Broussard, Y.U. Idzerda, M.S. Osofsky, R.J. Soulen, Jr., Epitaxial multilayers of ferromagnetic insulators with nonmagnetic metals and superconductors, Proc. SPIE 2157, Superconducting Superlattices and Multilayers, 285 (1994).

[65] P.M. Tedrow, J.E. Tkaczyk, A. Kumar, Spin-polarized electron tunneling study of an artificially layered superconductor with internal magnetic field: EuO-Al, Phys. Rev. Lett. 56, 1746 (1986).

[66] A.M. Van Diepen, H.W. De Wijn, K.H.J. Buscho, Nuclear Magnetic Resonance and Susceptibility of Equiatomic Rare-Earth-Aluminum Compounds, Phys. Stat. Sol. 29, 189 (1968).

[67] B. Li, N. Roschewsky, B.A. Assaf, M. Eich, M. Epstein-Martin, D. Heiman, M. Munzenberg, J.S. Moodera, Superconducting Spin Switch with Infinite Magnetoresistance Induced by an Internal Exchange Field, Phys. Rev. Lett. 110, 097001 (2013).

[68] H. Haugen, D. Huertas-Hernando, A. Brataas, Spin transport in proximity induced ferromagnetic graphene. Phys. Rev. B 77, 115406 (2008).

[69] A.D. Mohite, T.S. Santos, J.S. Moodera, B.W. Alphenaar, Observation of the triplet exciton in EuS-coated single-walled nanotubes, Nat. Nano. 4, 425 (2009).

[70] F. D. M. Haldane, Model for a Quantum Hall Effect without Landau Levels: Condensed-Matter Realization of the "Parity Anomaly", Phys. Rev. Lett. 61, 2015 (1988).

[71] H. Pan, Z. Li, C.C. Liu, G. Zhu, Z. Qiao, Y. Yao, Valley-Polarized Quantum Anomalous Hall Effect in Silicene, Phys. Rev. Lett. 112, 106802 (2014).

[72] Z. Qiao, W. Ren, H. Chen, L. Bellaiche, Z. Zhang, A.H. MacDonald, Qian Niu, Quantum Anomalous Hall Effect in Graphene Proximity Coupled to an Antiferromagnetic Insulator, Phys. Rev. Lett. 112, 116404 (2014).

[73] P. Wei, F. Katmis, B.A. Assaf, H. Steinberg, P. Jarillo-Herrero, D. Heiman, J.S. Moodera, Exchange-Coupling-Induced Symmetry Breaking in Topological Insulators, Phys. Rev. Lett. 110, 186807 (2013).

[74] C.Z Chang, J. Zhang, X. Feng, J. Shen, Z. Zhang, M. Guo, K. Li, Y. Ou, P. Wei, L.L. Wang, Z.Q. Ji, Y. Feng, S. Ji, X. Chen, J. Jia, X. Dai, Z. Fang, S.C. Zhang, K. He, Y. Wang, L. Lu, X.C. Ma, Q.K. Xue, Experimental Observation of the Quantum Anomalous Hall Effect in a Magnetic Topological Insulator, Science, 340, 167 (2013).

[75] J.D. Sau, R.M. Lutchyn, S. Tewari, S. Das Sarma, Generic New Platform for Topological Quantum Computation Using Semiconductor Heterostructures, Phys. Rev. Lett. 104, 040502 (2010).

[76] L. Fu and C.L. Kane, Superconducting Proximity Effect and Majorana Fermions at the Surface of a Topological Insulator, Phys. Rev. Lett. 100, 096407 (2008).

[77] A.C. Potter, P.A. Lee, Multichannel Generalization of Kitaev's Majorana End States and a Practical Route to Realize Them in Thin Films, Phys. Rev. Lett. 105, 227003 (2010).

[78] Y. Oreg, G. Refael, F. von Oppen, Helical liquids and Majorana bound states in quantum wires, Phys. Rev. Lett. 105, 177002 (2010).

[79] R.M. Lutchyn, T.D. Stanescu, S. Das Sarma, Search for Majorana Fermions in Multiband Semiconducting Nanowires, Phys. Rev. Lett. 106, 127001 (2011).

[80] J. Alicea, New directions in the pursuit of Majorana fermions in solid state systems, Rep. Prog. Phys. 75, 076501 (2012).

[81] V. Mourik, K. Zuo, S.M. Frolov, S.R. Plissard, E.P.A.M. Bakkers, L.P. Kouwenhoven, Signatures of Majorana fermions in hybrid superconductor-semiconductor nanowire devices, Science 336 (6084), 1003–1007 (2012).

[82] M.T. Deng, C.L. Yu, G.Y. Huang , M. Larsson , P. Caroff, H.Q. Xu, Anomalous Zero-Bias Conductance Peak in a Nb–InSb Nanowire–Nb Hybrid Device, Nano Lett., 12 (12), 6414–6419 (2012).

[83] A. Das, Y. Ronen, Y. Most, Y. Oreg, M. Heiblum, H. Shtrikman, Zero-bias peaks and splitting in an Al–InAs nanowire topological superconductor as a signature of Majorana fermions, Nature Physics 8, 887–895 (2012).

[84] S. Nadj-Perge, I.K. Drozdov, J. Li, H. Chen, S. Jeon, J. Seo, A.H. MacDonald, B.A. Bernevig, A. Yazdani, Observation of Majorana fermions in ferromagnetic atomic chains on a superconductor, Science 346(6209), 602-607 (2014).

[85] T.D. Stanescu, S. Tewari, Majorana fermions in semiconductor nanowires: fundamentals, modeling, and experiment, J. Phys.: Condens. Matter 25 233201 (2013).

[86] M.H. Freedman, A. Kitaev, M.J. Larsen, Z. Wang, Topological quantum computation, Bull. Amer. Math. Soc. 40, 31 (2003).

[87] C. Nayak, S.H. Simon, A. Stern, M. Freedman, S. Das Sarma, Non-Abelian anyons and topological quantum computation, Rev. Mod. Phys. 80, 1083 (2008).

[88] A.Yu. Kitaev, Fault-tolerant quantum computation by anyons, Anna. Phys. 303, 2 (2003).

[89] R. Raussendorf, J. Harrington, Fault-Tolerant Quantum Computation with High Threshold in Two Dimensions, Phys. Rev. Lett. 98, 190504 (2007).

[90] G.X. Miao, J. Chang, B.A. Assaf, D. Heiman, J.S. Moodera, Spin regulation in composite spin-filter barrier devices, Nat. Commun. 5, 3682 (2014).

[91] F. Giazotto, S. Bergeret, J.S. Moodera, J. Robinson, Proposal for a phase-coherent thermoelectric transistor, Appl. Phys. Lett. 105, 062602 (2014).

[92] D. P. DiVincenzo, Quantum computing and single-qubit measurements using the spin-filter effect (invited), J. Appl. Phys. 85, 4785 (1999).

[93] Y. Ohno, D.K. Young, B. Beschoten, F. Matsukura, H. Ohno, D.D. Awschalom, Electrical spin injection in a ferromagnetic semiconductor heterostructure, Nature 402, 790-792 (1999).

[94] B.T. Jonker, Y.D. Park, B.R. Bennett, H.D. Cheong, G. Kioseoglou, A. Petrou, Robust electrical spin injection into a semiconductor heterostructure, Phys. Rev. B 62, 8180 (2000).

[95] S.B. Ogale, Dilute Doping, Defects, and Ferromagnetism in Metal Oxide Systems, Adv. Mater. 22(29) 3125–3155 (2010).

[96] T. Dietl, A ten-year perspective on dilute magnetic semiconductors and oxides, Nature Materials 9, 965–974 (2010).

[97] A.H. MacDonald, P. Schiffer, N. Samarth, Ferromagnetic semiconductors: moving beyond (Ga,Mn)As, Nat. Mater. 4, 195 - 202 (2005).

[98] J.M.D. Coey, Dilute magnetic oxides, Current Opinion in Solid State and Materials Science 10(2) 83–92 (2006).

[99] K.S. Burch, D.D. Awschalom, D.N. Basov, Optical properties of III-Mn-V ferromagnetic semiconductors, J. Magn. Magn. Mater. 320(23), 3207–3228 (2008).

[100] T. Dietl, H. Ohno, Dilute ferromagnetic semiconductors: Physics and spintronic structures, Rev. Mod. Phys. 86, 187 (2014).

[101] F.D.M. Haldane, Model for a Quantum Hall Effect without Landau Levels: Condensed-Matter Realization of the "Parity Anomaly", Phys. Rev. Lett. 61, 2015 (1988).

[102] C.R. Dean, L. Wang, P. Maher, C. Forsythe, F. Ghahari, Y. Gao, J. Katoch, M. Ishigami, P. Moon, M. Koshino, T. Taniguchi, K. Watanabe, K.L. Shepard, J. Hone, P. Kim, Hofstadter's butterfly and the fractal quantum Hall effect in moiré superlattices, Nature 497, 598–602 (2013).

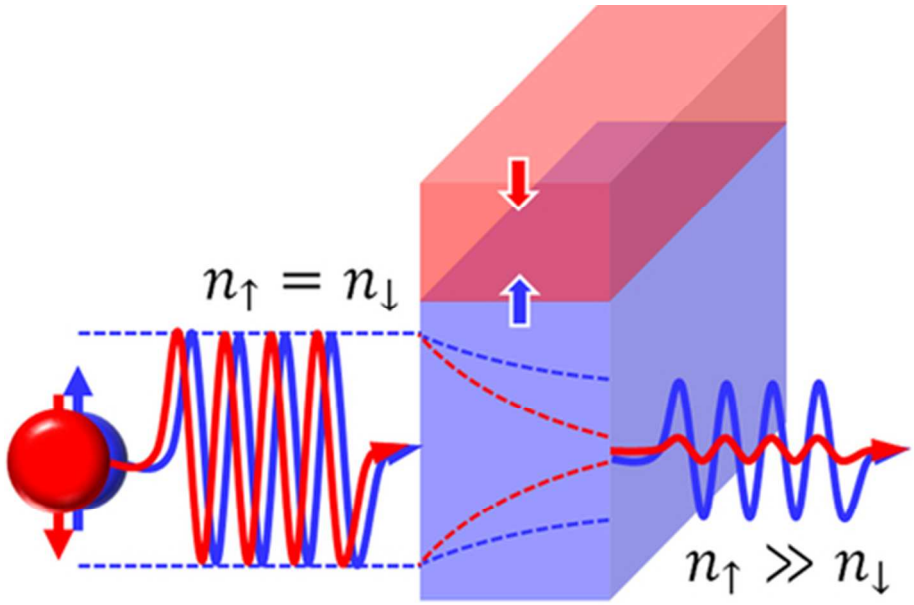

Magnetic semiconductors with unique spin-filtering property and ability to create excessive internal magnetic fields can open myriads of new phenomena.
39x25mm (300 x 300 DPI)